

Comprehensive Analysis To Assess And Remove Causes Of Decline Flow In An Offshore Compression Module.

Vladimir Alexis Neri Quezadas,

Abstract: In a three stages compression module, at an offshore installation, was detected a sudden decrease in managed flow, decreasing from 108 to 87 million standard cubic feet by day (MMSCFD). Thermodynamic analysis on performance of three stages of compression, axial compressor and power turbine was carried out. Each compression stage were found operating efficiently according to ranges indicated by manufacturer. However, a power loss about 1200 hp was detected in turbine, so that the problem between the power turbine and the main gearbox (MG) was focused. Boroscopic and thermographic inspections were carried out, detecting hot spots and contaminants deposition. Upon disassembling MG, lubrication ducts were detected partially obstructed by silicone.

Index Terms: Gas compression, analysis and troubleshooting, gas processing, gas turbine, thermography, performance test, gearbox, lubrication, compression efficiency.

1 INTRODUCTION.

Offshore compressor systems are critical equipment to handle gas production and ship it for its processing to inland shore complexes. Because of their greater capacity to handle medium-high gas flows [1], the use of gas turbine driven centrifugal type compressors is preferred. In oil installations in Mexico, compressors can be found operating over 20 years [2], so their monitoring and control systems are often obsolete or deficient. In this context, the development of techniques or procedures for the early detection of performance deficiencies in compressors and their components, which do not rely solely on instrumented systems, is an advantage to prevent unscheduled shutdowns, increase reliability and minimize gas flare. In this case the performance of a centrifugal compression train of 14 stages in total, three sections (low, medium and high pressure) is analyzed; divided between two compression bodies (first: model 6CDK37, second: model 8BK37), manufactured by Transamerica Delaval [3]. It is equipped with electric generator, main transmission and auxiliary transmission (for generator). The assembly is powered by a gas generator model LM-2500 PC and power turbine PGT25, manufactured by General Electric [4]. Each compression train has a gas power of 24,050 bhp @ 8,700 rpm and rated capacity to compress 90 MMscfd of bitter gas as shown in Figure 1. The first section holds 10 MMscfd, takes gas at a gauge pressure of 7.1 psi and discharge it at 66.8 psi, in the second section an additional gas flow is received for a capacity of 90 MMscfd, suction pressure at 59.7 psi discharge at 302.9 psi, finally in third section designed to handle 90 MMscfd, gas enters at a pressure of 293.0 psi and discharge at 1166.3 psi. Due to the decline of the oil fields, the composition of the gas has been modified from that of the design, reducing the average molecular weight of the gas at low pressure section from 34.8 (design) to 30.8 (current).

The molecular weight of the medium pressure gas section was reduced from 26.3 (design) to 24.0 (current). These molecular weight modifications, coupled with a reduction in the discharge pressure requirement to 995.6 psig, have resulted in an increase in gas handling capacity at 95 MMscfd for each train. From these operational changes an update was made on the performance curves of the centrifugal compressors at each section.

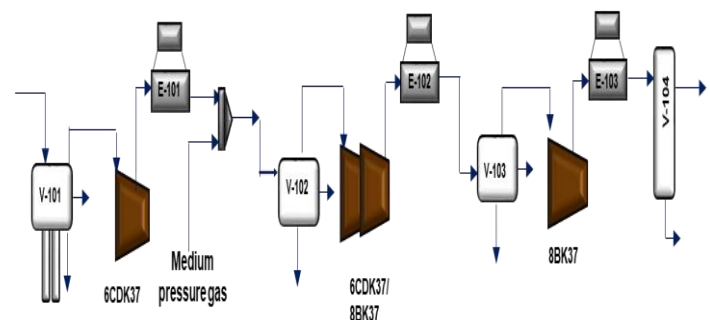


Fig. 1. Compressor train arrangement.

Annual maintenance was performed on compression train "B" and returned to normal operation handling a flow of 9.0 MMscfd in the first section and 94 MMscfd as total discharge. One week later the total discharge flow dropped suddenly to 87 MMscfd, without vibration, high temperature or component failure alarms. The gas flow measurement was verified as correct using a portable ultrasonic gauge with mean uncertainty of $\pm 0.3\%$. Due to this situation it was decided to use the thermodynamic analysis of compression train performance, starting from the operation data of the compression sections, power turbine and axial compressor. At the time of analysis the power turbine has 30131 hours and the gas generator 24155 hours of operation accumulated.

- ALEXIS NERI is a Senior Consultant at Petroexperts, leading dynamic simulation of O&G process facilities. Mr Neri has more than 15 years of expertise in turbomachinery and process simulation. He holds a BS degree in chemical engineering from Universidad Nacional Autonoma de Mexico (UNAM).

NOMENCLATURE:

b	First stage impeller exit width (ft)
f	Polytropic work factor
h	Enthalpy (Btu/lbm)
N	Rotative speed (rpm)

n	Polytropic exponent
ns	Isentropic exponent
Mw	Molecular weight
P	Pressure (psi)
Pg	Gas power
q	Gas flow (acfm, MMscfd)
rP	Pressure ratio
rV	Volume ratio
RA, RB, RC	Machine Reynolds number correction constant
Rem	Machine Reynolds number
T	Temperature (°R)
V	Volume (ft ³ /lbm)
v	Specific volume (ft ³ /lbm)
U	Velocity at the outer blade tip diameter (ft/sec)
W	Work per unit mass (ft lbf/lbm)
η	Efficiency
u	Kinematic viscosity of the gas at inlet conditions (ft ² /sec)

Subscripts

c	Fluid's critical point value
d	Compressor discharge conditions
i	Compressor inlet conditions
p	Polytropic
sp	Specified conditions
t	Test conditions

Superscript

()'	Condition at discharge pressure with entropy equal to inlet entropy
------	---

2 METHODOLOGY.

The methodology and equations used for calculating compressor performance are based on ASME PTC-10 [5] y PTC-22 (R2014) [6] standards. Temperature and flow pressure gauges calibrated with patterns traceable to NIST were used. For flow measurement, a Fluxus® G601 portable meter was used, mounted on the discharge line of the compression train. The equation of state used to determine the thermodynamic properties of the process fluids is the Peng Robinson equation, which fulfills the objective of generating models for the simulation of liquid-vapor equilibrium in systems composed of non-polar light hydrocarbon mixtures [7]. In order to expedite the calculations of thermodynamic properties and the location of the points of operation of the equipment, the current performance curves of the centrifugal compressors, in addition to the compositions of the different hydrocarbon streams, were entered into a commercial program of process simulation. The energy losses of the compressor shaft by radiation are considered negligible. During the entire test the recirculation valves of each compression section were kept fully closed. The procedure used to determine the thermodynamic parameters of performance, from the readings made on site, is as follows: The process gas used in the test is modeled as real gas ($Z \neq 1$). The operational parameters measured in the field during the performance tests are: suction (Pi) and discharge (Pd) pressure, suction (Ti) and discharge (Td) temperature of the compressor, speed of rotation (N) and current gas flow (q).

Table.1 Composition for gas at low, medium and high pressure sections (mol fraction).

Component	Low pressure gas	Medium pressure gas	High pressure gas
Methane	0.4740	0.6742	0.6794
Ethane	0.1535	0.1217	0.1226
Propane	0.1205	0.0664	0.0669
i-Butane	0.0202	0.0100	0.0101
n-Butane	0.0583	0.0256	0.0258
i-Pentane	0.0176	0.0071	0.0072
n-Pentane	0.0247	0.0097	0.0098
C ₆ group	0.0177	0.0060	0.0060
C ₇ group	0.0087	0.0021	0.0021
C ₈ group	0.0027	0.0004	0.0004
C ₉ group	0.0003	0.0000	0.0000
C ₁₀ group	0.0000	0.0000	0.0000
Nitrogen	0.0027	0.0036	0.0036
Carbon dioxide	0.0214	0.0244	0.0246
Hydrogen sulfide	0.0277	0.0268	0.0270
Water	0.0500	0.0220	0.0145

These parameters are processed including the calculation of thermodynamic properties for the operating point. During the taking of operation readings, equipment was maintained at an operating speed in the range of 7982 ± 5 rpm. The process gas compositions for the low, medium and high pressure sections are given in Table 1. Critical proprieties are included in Table 2.

Table.2 Critical proprieties for gas at low, medium and high pressure sections.

Properties	Unit	Low pressure gas	Medium pressure gas	High pressure gas
Mw		30.75	23.94	23.99
P _c	psia	1688.84	1598.39	1598.49
T _c	°R	599.59	487.61	486.86
V _c	ft ³ /lbm	1.8453	1.3681	1.3674

- The physicochemical properties of the process gas, fuel gas and air are determined to the operation of the compression train. From this data, the change in enthalpy, based on a base condition of 15.56°C (60°F) and 1 atm (14,696 psia), is calculated.
- The performance parameters are calculated for each compression section at the test points: flow rate / velocity (q/N), isentropic exponents (ns), polytropic exponents (n) polytropic head (Wp), polytropic efficiency (η_p) and gas power (Pg).

$$n_s = \ln\left(\frac{r_d}{r_i}\right) / \ln\left(\frac{r'_d}{r'_i}\right) \quad (1)$$

$$n = \ln(r_p) / \ln(r'_p) \quad (2)$$

$$W_p = f\left(\frac{n}{n_s}\right)(p_d v_d - p_i v_i) \quad (3)$$

$$\eta_p = \frac{W_p}{W_c} \quad (4)$$

$$P_g = \frac{W_p \cdot n_s}{v} \quad (5)$$

- c. Performance is expressed from dimensionless parameters and conversion of test conditions to design conditions is done.

$$W_0 = \left(\frac{q}{\dots} \right) = \left(\frac{q}{\dots} \right) \quad (6)$$

- d. The Reynolds number of the machine is corrected with the correction constants (RA, RB and RC). The number of Reynolds of the machine (Rem) per design for the first section of compression is 1.57x10⁷, for the second section is 5.47x10⁶ and for the third section is 1.22x10⁶.

$$Rem = Ub/v \quad (7)$$

$$RA = 0.066 + 0.934 \left| \frac{(4.8 \times 10^{-4} \times D)}{\dots} \right| \quad (8)$$

$$RB = \frac{\dots}{13.67} \quad (9)$$

$$RC = \frac{0.958}{\dots} \quad (10)$$

- e. Interpolation or extrapolation process is performed with the correction constants. The performance of the compressor at different design points is determined with the test points.
- f. The performance parameters are transferred to design conditions for the different test points and the current performance of the compressor is predicted against the design expected (updated by change of composition).
- g. From the performance parameters of the centrifugal compressors plus the mechanical losses, the work of compression exerted on the gas in each section of compression is determined. The sum of the work exerted in each section constitutes the total work of compression.
- h. Total power of the arrow is obtained by adding the total work of compression, the work used in auxiliary components (electric generator, lubrication pumps, etc.) and mechanical losses in turbine and axial compressor.
- i. The current performance parameters (dimensional and dimensionless), transferred to the design conditions, are compared against those of updated design parameters.

3 RESULTS AND DISCUSSION.

The average results of the thermodynamic performance calculations at a speed of 7982 rpm for each of the compression sections (low, medium and high pressure) are presented in Tables 3, 4 and 5. Also three plots with test and design points comparisons for each section are included in Figures 2, 3 and 4.

Table.3 Performance parameters for low pressure section.

Low pressure section, test at 7982 rpm				
Item	Parameter/unit	Test	Updated design	Difference absolute
1	Suction pressure, psia	33.2	33.2	0.0
2	Suction temperature, °R	559.2	559.2	0.0
3	Flow, MMscfd	8.3	8.3	0.0
4	Flow, acfm	2727	2696	31
5	Discharge pressure, psia	95.8	95.8	0.0
6	Discharge temperature, °R	699.0	696.3	2.7
7	Compression ratio	2.89	2.89	0.00
8	Politropic efficiency, %	59.92	60.75	0.83
9	Politropic head, ft	29720	29470	250

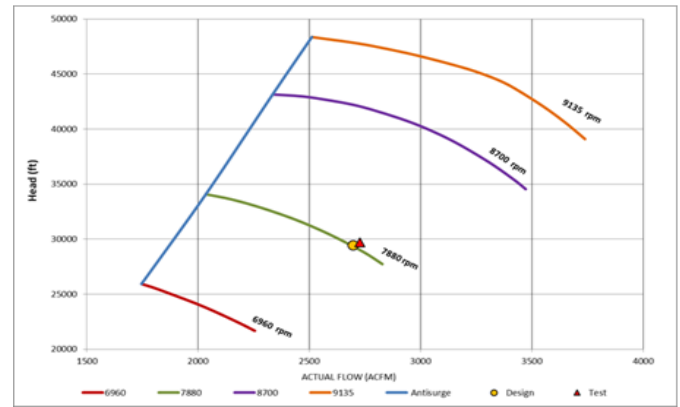


Fig. 2. Test and design performance at 7982 rpm for low pressure section.

Table.4 Performance parameters for medium pressure section.

Medium pressure section, test at 7982 rpm				
Item	Parameter/unit	Test	Updated design	Difference absolute
10	Suction pressure, psia	78.7	78.7	0.0
11	Suction temperature, °R	567.5	567.5	0.0
12	Flow, MMscfd	87.8	87.8	0.0
13	Flow, acfm	12180	12180	0
14	Discharge pressure, psia	296.3	299.2	2.9
15	Discharge temperature, °R	762.9	768.0	5.1
16	Compression ratio	3.77	3.80	0.03
17	Politropic efficiency, %	74.81	73.35	1.46
18	Politropic head, ft	55170	55690	520

According to the results obtained from the thermodynamic evaluation of each compression section, it is observed that the low and medium pressure stages operate at conditions similar to those of the updated design. Regarding design, there are deviations of less than 2% in polytropic efficiency.

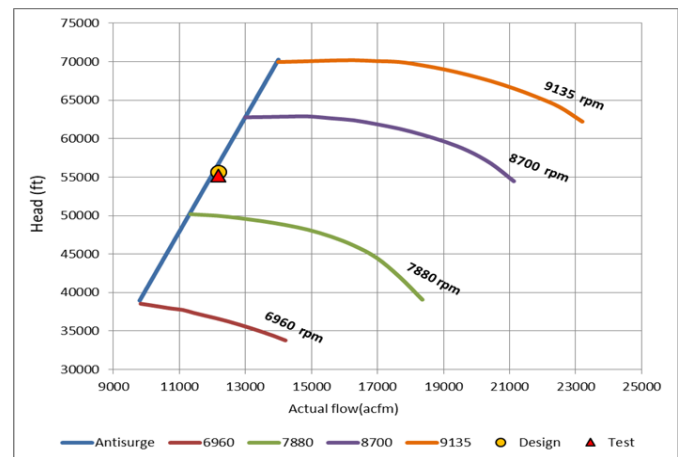


Fig. 3. Test and design performance at 7982 rpm for medium pressure section.

For the high pressure compression section, it was detected that there is an 8.6% increase in polytropic efficiency, so that the seal system, process instrumentation, surge control valves and pressure control systems were checked with the purpose of detecting and eliminating possible deviations in the readings of the compression train.

Table.5 Performance parameters for high pressure section.

High pressure section, test at 7982 rpm				
Item	Parameter/unit	Test	Updated design	Difference absolute
19	Suction pressure, psia	287.8	287.8	0
20	Suction temperature, °R	567.3	567.5	0.2
21	Flow, MMscfd	3128	3122	6
22	Flow, acfm	12180	12180	0
23	Discharge pressure, psia	872.3	878.0	5.7
24	Discharge temperature, °R	732.0	751.2	19.2
25	Compression ratio	3.03	3.05	0.10
26	Polytropic efficiency, %	75.60	67.00	8.6
27	Polytropic head, ft	43290	42260	1030

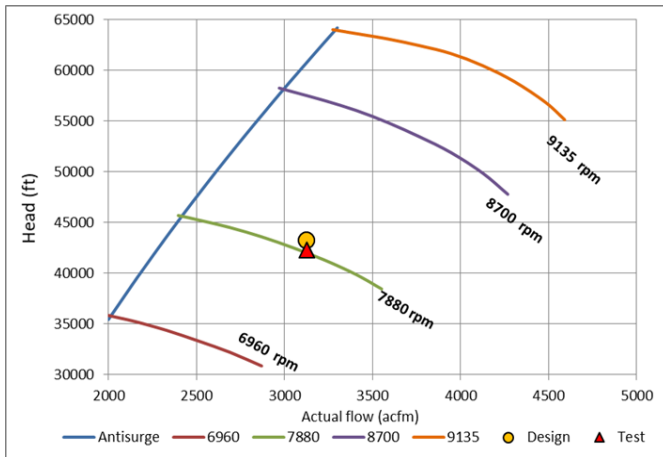


Fig. 4. Test and design performance at 7982 rpm for high pressure section.

The gas power for each of the compression sections plus the power used for the electric generation in the compression train is shown in Table 6. The total power supplied by the turbine as a useful work is 16322 hp. The power that should receive the compression train according to the curves of performance and process simulation is 17554 hp, so there is a difference of 1232 hp.

Table.6 Useful work provided by turbine to each compression section at NPT = 2935 rpm (compressor 7982 rpm).

Source	Low pressure, hp	Medium pressure, hp	High pressure, hp	Electric generator, hp	Total, hp
Test	781	8611	6530	400	16322
Updated design	755	8867	7532	400	17554
Difference	26	-256	-1002	0	-1232

Historical records of other compression equipment (trains A and C) operating under conditions similar to those of the train under analysis indicate that the average useful power recorded during tests was 18257 hp for train A and 18645 hp for train B, so the 17554 hp log on the analyzed equipment is considered abnormal. From this detected difference, the problem of compression train performance in the power turbine and / or the main gearbox was focused. Thermal imaging of these sections was carried out, in a second stage it was proposed to perform a boroscopic inspection of the

turbine and axial compressor. The thermographic images of the combustion chamber and the gas conductor indicate some hot spots at the turbine inlet, with no flue gas escaping to the flare, so this anomaly was ruled out as the cause of the power loss. The hot spots were subsequently analyzed, with loss of thickness in the material of the gas conductor. The thermographic images of the gearbox in its coupling with the first compression body (6CDK37) show a high temperature section (83 to 84 °C) in the bearing, at normal operating temperature for this section is 55 to 60 °C during normal operation. Based on these results the decision was taken to stop the operation of the compression train and to intervene the bearing of the coupling between the main gearbox and the compressor.

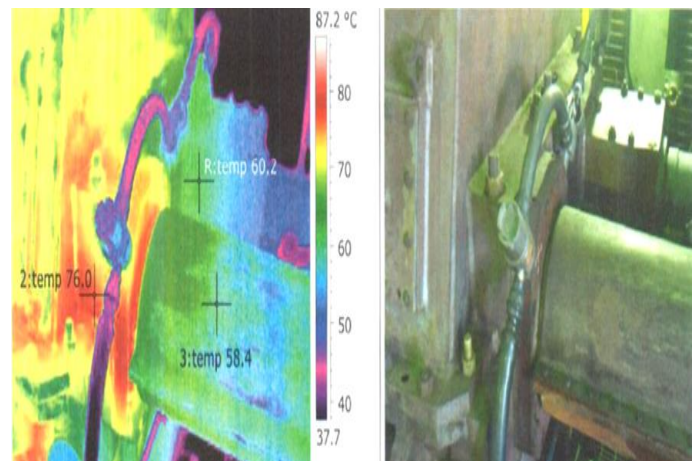


Fig. 5. Main gear thermographic image (turbine side).

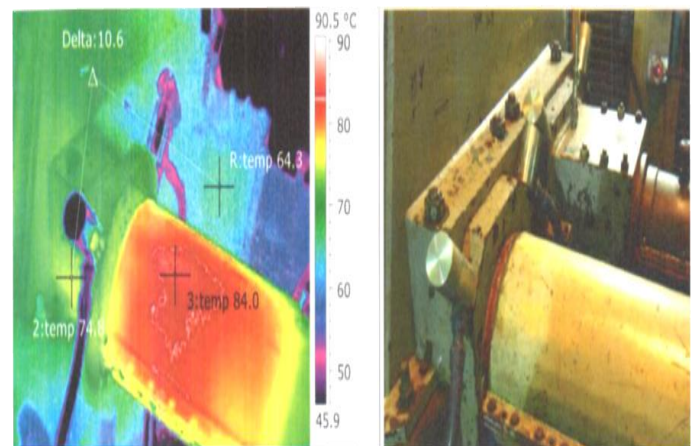


Fig. 6. Main gear thermographic image (compressor coupling side).

During the inspection and cleaning work, a portion of silicone was found blocking the sprinkler that lubricates the bell gears and nipples on main gearbox side. Sludge formed by mineral oil deteriorated by high temperature was also found. After the maintenance activities were completed, the compression train returned to operation, recording an average discharge flow of 94 MMscfd, which represents a recovery of 7 MMscfd. Further calculations on turbine performance indicate that useful work supplied by the turbine increased to a total of 18670 hp.

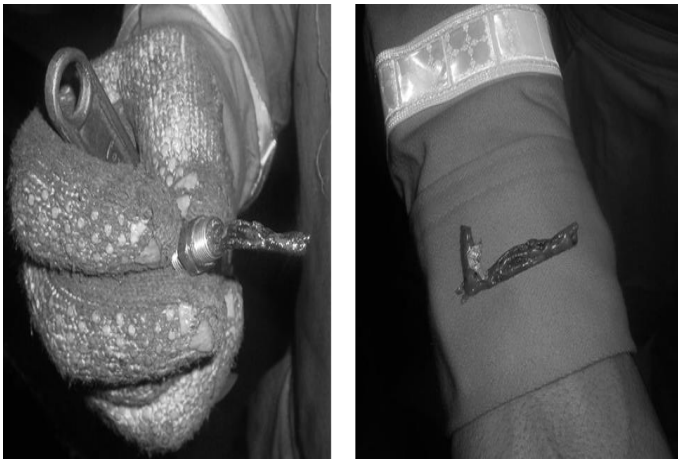


Fig. 6. Silicone portion finded at lubricant sprinkler.

4 CONCLUSION.

The combined use of thermodynamic analysis of compressor performance and preventive maintenance techniques increases the success rate in detecting root causes of rotating equipment anomalies. One of the most important advantages is limiting the possible causes of failures, which reduces the time elapsed between the detection of the deviation and the elimination of the origin cause. Rotating equipment operators must be alert to detect and report decreases in flow or pressure, helping to prevent component damage from increasing or extending to other sections. Multiple deviations from the process precede the occurrence of vibration and subsequent damage to unscheduled components or shutdowns.

REFERENCES

- [1] Royce N. Brown, "Compressors selection an sizing", Second Edition, Gulf Professional Publishing, 1997.
- [2] Petroleos Mexicanos, "Contexto operacional centro de proceso Pol-A", 2012.
- [3] Transamerica Delaval Inc, "Instructions single lift compressor trains", 1980.
- [4] Nuovo Pignone S.p.A., "GE Gas turbines", 2006.
- [5] ASME, "Performance Test Code on Compressors and Exhausters, PTC-10", 1997 (Reaffirmed 2014).
- [6] ASME, "Performance Test Code for Gas Turbines, PTC-22", 2014.
- [7] Nicolás José Scenna y col., "Modelado, simulación y optimización de procesos químicos", ISBN: 950-42-0022-2 ,1999.